PHYSICAL REVIEW B **96**, 064434 (2017)

Charge and spin order in $Ca_{0.5}Bi_{0.5}FeO_3$: Idle spins and frustration in the charge-disproportionated state

Fabio Denis Romero,[1,*] Yoshiteru Hosaka,[1] Noriya Ichikawa,[1] Takashi Saito,[1] Graham McNally,[2]
J. Paul Attfield,[2] and Yuichi Shimakawa[1,†]
[1]*Institute for Chemical Research, Kyoto University, Gokasho, Uji, Kyoto 611-0011, Japan*
[2]*Centre for Science at Extreme Conditions and School of Chemistry, The University of Edinburgh, Edinburgh EH9 3JZ, United Kingdom*

(Received 27 March 2017; revised manuscript received 1 August 2017; published 29 August 2017)

The perovskite $Ca_{0.5}Bi_{0.5}FeO_3$ undergoes a remarkable sequence of charge-disproportionation (CD) and charge-transfer (CT) transitions on cooling due to competing electronic instabilities: $Ca_{0.5}{Bi^{3+}}_{0.5}Fe^{3.5+}O_3 \rightarrow Ca_{0.5}{Bi^{3+}}_{0.5}{Fe^{3+}}_{0.67}{Fe^{4.5+}}_{0.33}O_3$ (CD phase) $\rightarrow Ca_{0.5}{Bi^{3+}}_{0.25}{Bi^{5+}}_{0.25}Fe^{3+}O_3$ (CT phase). The accompanying changes in charge and spin ordering have been determined from neutron diffraction and physical property measurements. The CT phase adopts a simple G-type antiferromagnetic structure of Fe^{3+} spins but the CD phase adopts an unusual charge and magnetic arrangement in which Fe^{3+} spins are antiferromagnetically ordered but the $Fe^{4.5+}$ moments have no long-range order due to magnetic frustration and form a spin glass at low temperatures.

DOI: 10.1103/PhysRevB.96.064434

I. INTRODUCTION

Materials in which structural, magnetic, and electronic transitions are coupled enable the fundamental solid-state physics of complex electronic orders to be investigated, and may lead to the development of multifunctional devices. One way to realize materials exhibiting coupled transitions is to prepare materials with transition metals in unusually high valence states via the use of strong oxidizing atmospheres. These materials can undergo charge transitions in order to relieve their electronic instabilities and these are typically accompanied by drastic changes to the transport, magnetic, and lattice properties [1].

Unusually high-valent transition-metal ions in ABO_3 perovskite-related oxides have been the subject of significant attention due to the rich variety of physical properties they can display [2–8]. These materials are of particular interest as their inherent electronic instabilities are often relieved via charge disproportionation (CD): on cooling $CaFeO_3$ and $CaCu_3Fe_4O_{12}$, the B-site Fe^{4+} disproportionates to Fe^{3+} and Fe^{5+}, which are charge ordered in a rock-salt-type manner, accompanied by a metal-insulator transition and a simultaneous transition to a ferrimagnetic state in $CaCu_3Fe_4O_{12}$ [9–11]. In $LaCu_3Fe_4O_{12}$ and $BiNiO_3$, on the other hand, the electronic instability of the high-valent $Fe^{3.75+}$ and Ni^{3+}, respectively, is relieved via intermetallic charge transfer (CT): $4Fe^{3.75+} + 3Cu^{2+} \rightarrow 4Fe^{3+} + 3Cu^{3+}$ and $Bi^{3+} + Ni^{3+} \rightarrow \frac{1}{2}Bi^{5+} + \frac{1}{2}Bi^{3+} + Ni^{2+}$ [2,12,13]. In both materials the CT is not only accompanied by significant changes to the magnetic and transport properties but also by a significant volume expansion on cooling below the CT transition temperature, while the latter material also reflects the CD instability of $Bi^{4+} : Bi^{4+} \rightarrow \frac{1}{2}Bi^{5+} + \frac{1}{2}Bi^{3+}$ [2,12,13].

The perovskite $Ca_{0.5}Bi_{0.5}FeO_3$ has recently been reported to contain unusually high-valent $Fe^{3.5+}$ and to undergo sequential charge transitions on cooling due to competing charge instabilities [14]. Magnetic and transport properties show significant anomalies associated with the charge transitions.

At 250 K there is a first-order transition from $Ca_{0.5}{Bi^{3+}}_{0.5}Fe^{3.5+}O_3$ to a CD state that can best be described as $Ca_{0.5}{Bi^{3+}}_{0.5}{Fe^{3+}}_{0.67}{Fe^{4.5+}}_{0.33}O_3$. Below approximately 200 K, intermetallic CT between A-site Bi and B-site Fe leads to the formation of $Ca_{0.5}{Bi^{3+}}_{0.25}{Bi^{5+}}_{0.25}Fe^{3+}O_3$. This transition is coupled to a colossal volume expansion on cooling below the transition temperature. Below this temperature, the CD and CT phases coexist and the ratio between the two is highly dependent on both the temperature and the cooling rate. The oxidation states of iron and the charge compositions of all three phases were confirmed by Mössbauer spectroscopy.

In this study we present detailed analysis of the crystal and magnetic structures of this material with neutron powder diffraction data in order to determine the charge and spin orders in the CD and CT phases. An unusual partial magnetic order with "idle" $Fe^{4.5+}$ spins is discovered in the CD phase.

II. EXPERIMENTAL

A polycrystalline sample of $Ca_{0.5}Bi_{0.5}FeO_3$ was obtained from a solid-state reaction under high-pressure and high-temperature conditions. Suitable stoichiometric amounts of $CaCO_3$, Bi_2O_3, and Fe_2O_3 were mixed and calcined at 650 °C in air. The calcined powder was sealed in a Pt capsule with $KClO_4$ as an *in situ* oxygen source, heated to 1100 °C under 5.3 GPa, and held for 30 min, followed by quenching to room temperature. The pressure was slowly released to ambient conditions after cooling. Finally, the obtained powder was washed with distilled water in order to remove residual KCl and $KClO_4$ and dried.

Laboratory x-ray powder diffraction data were collected using a Bruker D8 diffractometer using Cu $K\alpha$ radiation. Neutron powder diffraction data were collected using the GEM diffractometer at ISIS Neutron Source, United Kingdom, from a sample contained within a vanadium can. Rietveld refinements were performed using the GSAS suite of programs [15]. Mössbauer spectroscopy measurements were carried out in transmission geometry with a constant-acceleration

---

[*] fabio.denis.74n@st.kyoto-u.ac.jp

[†] shimak@scl.kyoto-u.ac.jp

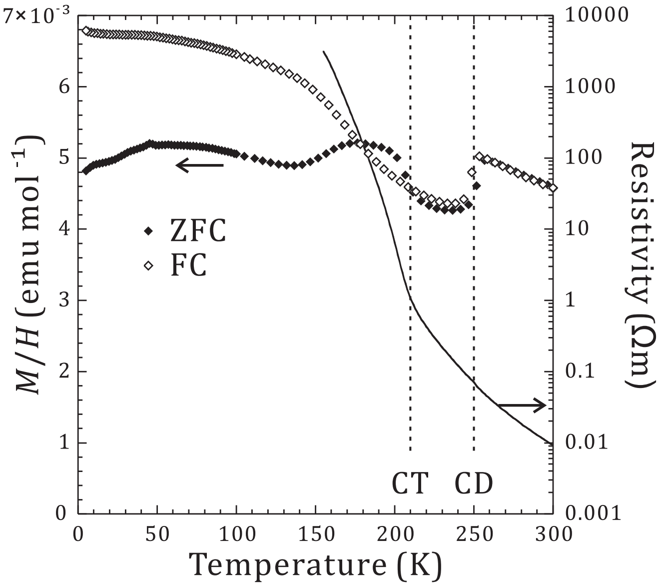

FIG. 1. Zero-field and field-cooled magnetization data and resistivity data collected as a function of temperature from $Ca_{0.5}Bi_{0.5}FeO_3$.

spectrometer using a 57 Co/Rh radiation source and were fitted with Lorentzian functions. Magnetic properties were measured with a commercial Quantum Design MPMS superconducting quantum interference device magnetometer.

III. RESULTS

X-ray powder diffraction data confirmed the as-synthesised $Ca_{0.5}Bi_{0.5}FeO_3$ sample was single phase and crystallizes in the *Pnma* structure previously reported [14]. Magnetization and resistivity data collected as a function of temperature show two anomalies consistent with successive CD and intermetallic CT transitions (Fig. 1).

The structural model previously reported [space group *Pnma*, $a = 5.5122(6)$ Å, $b = 7.7042(9)$ Å, and $c = 5.4024(6)$ Å, Fig. 2(a)] was successfully refined against neutron powder diffraction data collected at 300 K to give good calculated and observed fits [$\chi^2 = 4.906$, Fig. 3(a)]. Details of the refined structure are given in the Supplemental Material [16]. The *A* sites are randomly occupied by Bi and Ca and the oxygen sites are fully occupied, confirming the $Ca^{2+}{}_{0.5}Bi^{3+}{}_{0.5}Fe^{3.5+}O_3$ composition. The lack of additional magnetic reflections in the neutron powder diffraction data between 300 and 250 K is consistent with paramagnetic Fe, as suggested by magnetization data for the high-temperature state $Ca_{0.5}Bi^{3+}{}_{0.5}Fe^{3.5+}O_3$ and the single paramagnetic signal observed in Mössbauer spectroscopy data collected at 300 K [14].

Neutron powder diffraction data collected as a function of temperature on cooling from 300 to 5 K in 10-K steps showed the same structural transitions observed in previous synchrotron powder diffraction data [14]. Both structural transitions were accompanied by the appearance of additional reflections in the neutron powder diffraction data [Figs. 3(b) and 3(c)].

Reflections of the main phase at 240 K, below the CD transition temperature, are consistent with the charge disproportionation of $Ca_{0.5}Bi^{3+}{}_{0.5}Fe^{3.5+}O_3$ to $Ca_{0.5}Bi^{3+}{}_{0.5}Fe^{3+}{}_{0.67}Fe^{4.5+}{}_{0.33}O_3$. The additional reflections could be indexed on the basis of a magnetic cell corresponding to a $1 \times 1 \times 3$ expansion of the nuclear cell. The best fit to the data ($\chi^2 = 2.914$) was achieved with a layered arrangement of charge and spins with the *c* axis as the stacking direction as shown in Fig. 2(b). Two out of every three Fe layers are ordered antiferromagnetically within and between layers with a moment of $3.02(2)\,\mu_B$ per Fe center at 5 K. The best fit to the data was achieved using a model in which these spins are aligned along the *b* axis. The remaining Fe layer does not contribute any magnetic scattering, consistent with the paramagnetic component observed in the Mössbauer spectroscopy data collected at this temperature [14].

This magnetic structure is compatible with the 2:1 ratio of Fe^{3+}:$Fe^{4.5+}$ and provides evidence that the Fe cations are charge ordered with two antiferromagnetically ordered Fe^{3+} layers for every one paramagnetic $Fe^{4.5+}$ layer. An attempt was made to refine a nuclear cell of the same dimensions as the magnetic cell against the neutron powder diffraction data to determine oxygen displacements associated with charge ordering of Fe^{3+} and $Fe^{4.5+}$ but the resulting refinement was not stable and did not result in an improvement of the fit to the data. This is likely due to the fact that charge ordering is accompanied by only very small modifications to the oxygen positions. Observed, calculated, and difference plots are shown in Fig. 3(b) and details of the refined structure are given in the Supplemental Material [16].

As previously reported from synchrotron x-ray powder diffraction data, data collected below ~200 K result from a mixture of the CD and CT phases [14]. Neutron powder diffraction data collected below 200 K show additional

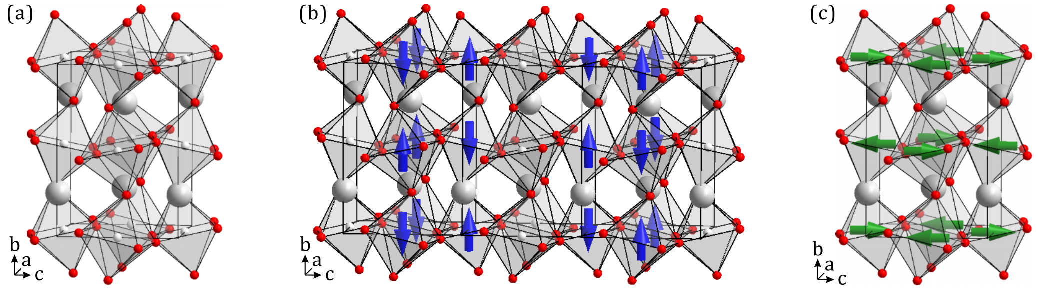

$Ca_{0.5}Bi^{3+}_{0.5}Fe^{3.5+}O_3$ $Ca_{0.5}Bi^{3+}_{0.5}Fe^{3+}_{0.67}Fe^{4.5+}_{0.33}O_3$ $Ca_{0.5}Bi^{3+}_{0.25}Bi^{5+}_{0.25}Fe^{3+}O_3$

FIG. 2. Refined structures of the three phases of $Ca_{0.5}Bi_{0.5}FeO_3$ showing the Fe spin orders in the two low-temperature phases.

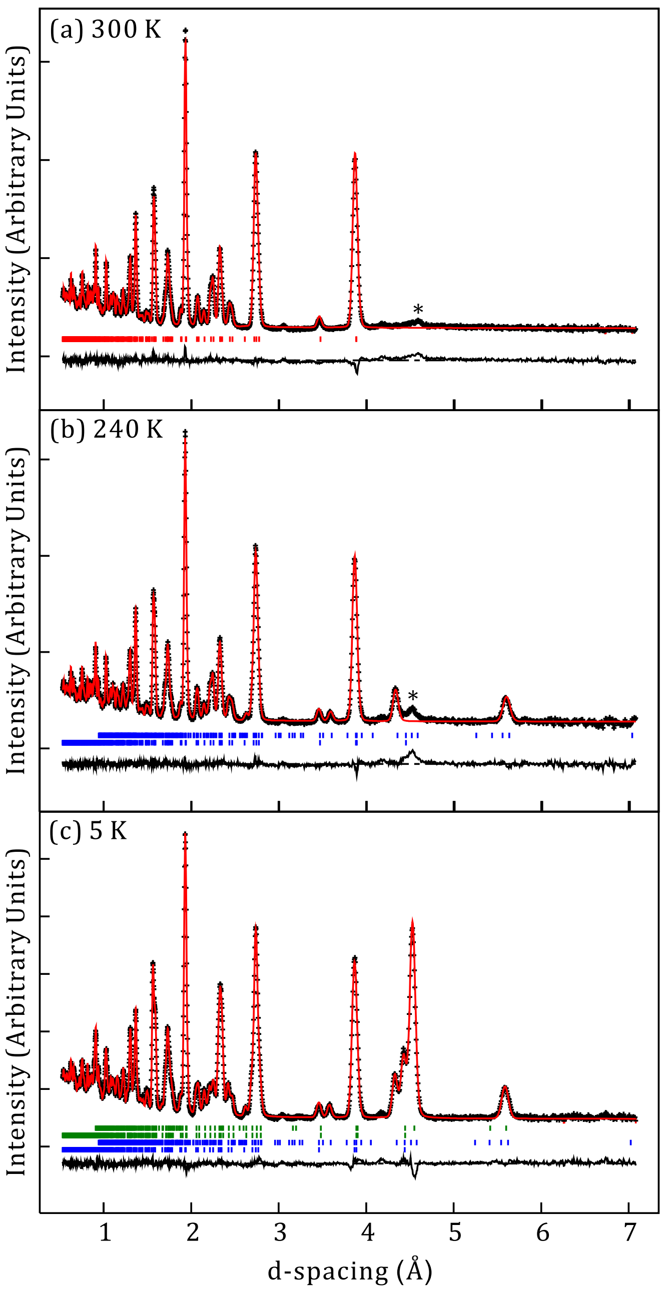

FIG. 3. Observed, calculated, and difference plot for the refinement of $Ca_{0.5}Bi_{0.5}FeO_3$ against neutron powder diffraction data collected at: (a) 300 K. The red tick marks correspond to contributions from the high-temperature phase $Ca_{0.5}Bi^{3+}{}_{0.5}Fe^{3.5+}O_3$. The unindexed featured marked with the asterisk is a contribution from a trace of Fe_2O_3 (<0.2% by weight). (b) 240 K. The upper set of tick marks correspond to magnetic reflections and the lower to nuclear reflections of the CD phase $Ca_{0.5}Bi^{3+}{}_{0.5}Fe^{3+}{}_{0.67}Fe^{4.5+}{}_{0.33}O_3$. The feature marked with the asterisk contains a small contribution from the CT phase $Ca_{0.5}Bi^{3+}{}_{0.25}Bi^{5+}{}_{0.25}Fe^{3+}O_3$ (see Supplemental Material) [16]. (c) 5 K. From top to bottom the tick marks correspond to magnetic and nuclear reflections of the CT phase $Ca_{0.5}Bi^{3+}{}_{0.25}Bi^{5+}{}_{0.25}Fe^{3+}O_3$ and magnetic and nuclear reflections of the CD phase $Ca_{0.5}Bi^{3+}{}_{0.5}Fe^{3+}{}_{0.67}Fe^{4.5+}{}_{0.33}O_3$.

reflections compared to those at 240 K consistent with the presence of the CT phase $Ca_{0.5}Bi^{3+}{}_{0.25}Bi^{5+}{}_{0.25}Fe^{3+}O_3$. These reflections can be indexed on the basis of a magnetic cell with the same dimensions as the nuclear cell. No additional features suggesting ordering of Bi^{3+} and Bi^{5+} were observed. The best fit to the data collected at 5 K ($\chi^2 = 4.203$) was achieved with a G-type antiferromagnetic arrangement of spins [4.29(2) μ_B at 5 K] pointing along the c direction [Fig. 2 (c)]. Observed, calculated, and difference plots are shown in Fig. 3(c) and details of the refined structure are given in the Supplemental Material [16].

Refined lattice parameters, unit-cell volume, phase fractions, and magnetic moments refined against neutron powder diffraction data collected as a function of temperature are given in the Supplemental Material [16].

IV. DISCUSSION

The charge disproportionation and the ordering of Fe^{3+} and $Fe^{4.5+}$ in the CD phase are unusual. CD transitions of unusually high-valent Fe usually produce Fe^{3+} (d^5) and Fe^{5+} ($d^5\underline{L}^2$) as a result of ligand hole ($\underline{L}$) localization due to strong hybridization between low-lying Fe $3d$ and O $2p$ orbitals [17,18]. Full charge disproportionation of $Fe^{3.5+}$ present in $Ca_{0.5}Bi_{0.5}FeO_3$ at 250 K was expected to result in a 3:1 ratio of Fe^{3+} and Fe^{5+} as observed in $CeCu_3Fe^{3.5+}{}_4O_{12}$ [4].

The 2:1 charge-disproportionated Fe^{3+} and $Fe^{4.5+}$ show charge ordering (CO) as evidenced by the arrangement of spins in the refined magnetic structure. This is in contrast to $CeCu_3Fe^{3.5+}{}_4O_{12}$, which exhibits charge disproportionation but not charge ordering [4]. One possible explanation for the unusual CD and CO behavior exhibited by $Ca_{0.5}Bi_{0.5}FeO_3$ can be reached by considering the possible symmetry modifications involved in the adoption of a charge-ordered structure. Other reported materials containing high-valent Fe centers that show charge disproportionation do so either to a charge-disordered state that is isosymmetric (e.g., $CeCu_3Fe^{3.5+}{}_4O_{12}$) or to one of the parent structure's maximal subgroups in order to minimize the disruption caused by these electronic changes [4,10,11,19].

The high-temperature structure of $Ca_{0.5}Bi_{0.5}FeO_3$ is a simple $GdFeO_3$-type perovskite (space group *Pnma*). Neither it nor any of its maximal subgroups can accommodate a 3:1 arrangement of Fe^{3+} and Fe^{5+}. However, one of its maximal isomorphic subgroups is a *Pnma* cell with an expansion of $a' = a, b' = b$, and $c' = 3c$ (where a', b', c' and a, b, c are the unit-cell dimensions of the subgroup and its parent space group, respectively) which can accommodate two symmetry-independent iron sites in a 2:1 ratio and can be used to replicate the charge-ordering pattern observed in the neutron powder diffraction data. In $Ca_{0.5}Bi_{0.5}FeO_3$, CD and CO with a 2:1 arrangement of Fe^{3+} and $Fe^{4.5+}$ is thus adopted instead of the 3:1 arrangement of Fe^{3+} and Fe^{5+} in order to minimize the lattice disruption. The presence of mixed-valent $Fe^{4.5+}$ explains why the CD transition at 250 K is not associated with a significant change in the resistivity of $Ca_{0.5}Bi_{0.5}FeO_3$ (Fig. 1).

In $Ca_{0.5}Bi^{3+}{}_{0.5}Fe^{3+}{}_{0.67}Fe^{4.5+}{}_{0.33}O_3$, two-thirds of the B sites are occupied by Fe^{3+} which are coupled antiferromagnetically to their nearest-neighbor Fe^{3+} centers [Fig. 2(b)]. This implies that J_1, the nearest-neighbor interaction between adjacent high-spin d^5 Fe^{3+} centers, is very large and antiferromagnetic as expected from simple Goodenough-Kanamori rules applied to two adjacent high-spin d^5 Fe^{3+} centers

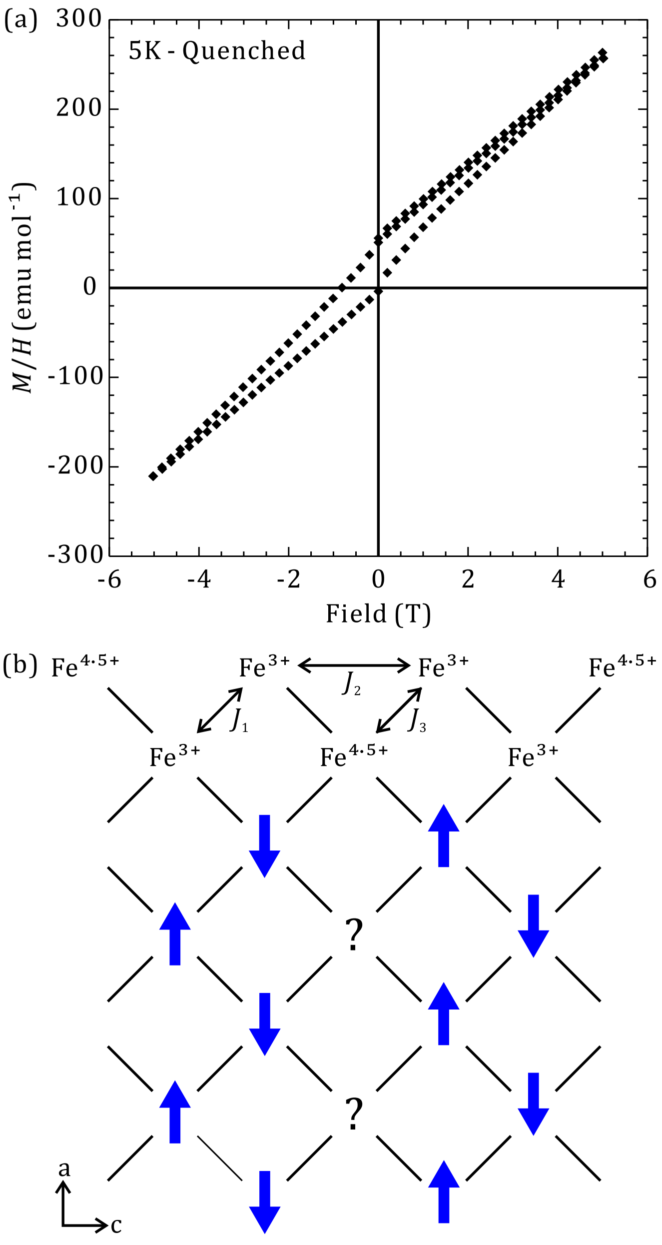

FIG. 4. (a) Field-cooled M/H curve collected from $Ca_{0.5}Bi^{3+}{}_{0.5}Fe^{3+}{}_{0.67}Fe^{4.5+}{}_{0.33}O_3$. (b) Relative orientations of the magnetic moments in the ac plane of $Ca_{0.5}Bi^{3+}{}_{0.5}Fe^{3+}{}_{0.67}Fe^{4.5+}{}_{0.33}O_3$.

[Fig. 4(b)] [20]. J_2, the next-nearest-neighbor interaction between Fe^{3+} centers, is also strong and antiferromagnetic, accounting for the pairs of centers on either side of a given paramagnetic site being aligned antiparallel to each other. Such a long-distance magnetic interaction is also present in other oxide materials containing unusually high-valent Fe centers and often induces nontrivial magnetic structures as a result of competing magnetic interactions [10,21–23]. The arrangement of Fe^{3+} spins around each $Fe^{4.5+}$ site results in magnetic frustration within the ac planes [Fig. 4(b)] regardless of the sign of J_3, the nearest-neighbor interaction between Fe^{3+} and $Fe^{4.5+}$ sites. Long-distance magnetic interactions are also expected between $Fe^{4.5+}$ spins along the b axis, which would generate competing magnetic interaction in this direction.

The magnetic structure adopted by the CD phase, in which only some of the magnetic sites order, is similar to that previously observed in materials such as $Fe_3F_8(H_2O)_2$ and $MnFe_2F_8(H_2O)_2$ [24]. $Fe_3F_8(H_2O)_2$ contains a 2:1 ratio of $Fe^{2+} : Fe^{3+}$ on a triangular lattice and is magnetically frustrated. Consequently, at the magnetic transition temperature ($T_N \approx 160$ K) only the Fe^{3+} spins order while the Fe^{2+} are "idle" and remain paramagnetic down to a second ordering temperature ($T_N \approx 40$ K) [24]. In $Ca_{0.5}Bi^{3+}{}_{0.5}Fe^{3+}{}_{0.67}Fe^{4.5+}{}_{0.33}O_3$ the $Fe^{4.5+}$ spins are similarly idle and the two layers on either side are ordered antiparallel to each other. The refined saturated magnetic moment of $3.02(2)\,\mu_B$ for this phase is slightly lower than expected for high-spin d^5 Fe^{3+} but higher than that of a mixed Fe^{3+}/Fe^{5+} site such as those found in $CeCu_3(Fe^{3+}{}_{0.75}Fe^{5+}{}_{0.25})_4O_{12}$ [$2.27(4)\,\mu_B$] [4]. This is not a surprising result given the presence of magnetic frustration in this system.

Mössbauer data collected at 5 K do not contain any paramagnetic component [14]. A field-cooled hysteresis loop collected at 5 K from a rapidly cooled sample (in which the CD phase is kinetically trapped) is offset from the origin [Fig. 4(a)], indicating the freezing of the idle spins at a temperature between 5 and 240 K and spin-glass behavior from the $Fe^{4.5+}$ sites. Determination of the spin-glass freezing temperature is challenging due to the contribution of the CT phase $Ca_{0.5}Bi^{3+}{}_{0.25}Bi^{5+}{}_{0.25}Fe^{3+}O_3$ to the magnetic data.

The CD phase $Ca_{0.5}Bi^{3+}{}_{0.5}Fe^{3+}{}_{0.67}Fe^{4.5+}{}_{0.33}O_3$ is unstable with respect to intermetallic charge-transfer transition between A-site Bi and B-site Fe at 200 K. The CT phase is a simple perovskite oxide containing only high-spin d^5 Fe^{3+}, isoelectronic and isostructural to the orthoferrites ($AFe^{3+}O_3$, $A =$ Ln, Y) which typically adopt simple G-type antiferromagnetic structures with saturated magnetic moments of approximately $\sim 4.5-4.7\,\mu_B$ and very high ordering temperatures ($T_N > 600$ K) [25,26]. $Ca_{0.5}Bi^{3+}{}_{0.25}Bi^{5+}{}_{0.25}Fe^{3+}O_3$ shows similar behavior with a simple G-type antiferromagnetic structure with a saturated moment of $4.29(2)\,\mu_B$ at 5 K [25].

In both the CD and CT phases, the refined moments almost immediately reach the 5-K saturated value following the charge transitions. It is therefore extremely likely that the intrinsic T_N's of the CD and CT phases are significantly higher than 250 K as observed in $LaCu_3Fe_4O_{12}$ [2,27].

V. CONCLUSION

In conclusion, both of the sequential phase transitions in $Ca_{0.5}Bi_{0.5}FeO_3$ are coupled to magnetic ordering transitions. The first transition due to charge disproportionation of $Fe^{3.5+}$ to a 2:1 ratio of Fe^{3+} and $Fe^{4.5+}$ results in the adoption of an unusual magnetic structure in which only the Fe^{3+} spins are magnetically ordered while the $Fe^{4.5+}$ sites are frustrated and remain paramagnetic with spin-glass behavior at low temperature. The second, due to charge transfer between A-site Bi and B-site Fe to form $Ca_{0.5}Bi^{3+}{}_{0.25}Bi^{5+}{}_{0.25}Fe^{3+}O_3$, is coupled to the adoption of G-type antiferromagnetic order.

ACKNOWLEDGMENTS

This work was supported by JSPS Grants-in-Aid for Scientific Research (Grants No. 16H00888 and No. 16H02266), by a JSPS-EPSRC Core-to-Core program (A) Advanced Research Networks, by a grant for the Joint Project of Chemical Synthesis Core Research Institutions from MEXT, by the JST-CREST program of Japan, and by grants from the EPSRC. Support was also provided by the Royal Society. We thank STFC for the provision of ISIS beamtime, and Dr. Ivan da Silva for assistance with data collection.

[1] Y. Shimakawa, J. Phys. D: Appl. Phys. **48**, 504006 (2015).

[2] Y. W. Long, N. Hayashi, T. Saito, M. Azuma, S. Muranaka, and Y. Shimakawa, Nature (London) **458**, 60 (2009).

[3] I. Yamada, K. Tsuchida, K. Ohgushi, N. Hayashi, J. Kim, N. Tsuji, R. Takahashi, M. Matsushita, N. Nishiyama, T. Inoue, T. Irifune, K. Kato, M. Takata, and M. Takano, Angew. Chemie Int. Ed. **50**, 6579 (2011).

[4] I. Yamada, H. Etani, M. Murakami, N. Hayashi, T. Kawakami, M. Mizumaki, S. Ueda, H. Abe, K.-D. Liss, A. J. Studer, T. Ozaki, S. Mori, R. Takahashi, and T. Irifune, Inorg. Chem. **53**, 11794 (2014).

[5] S. Kojima, J. Nasu, and A. Koga, Phys. Rev. B **94**, 045103 (2016).

[6] M. Naka, H. Seo, and Y. Motome, Phys. Rev. Lett. **116**, 056402 (2016).

[7] A. Lebon, P. Adler, C. Bernhard, A. V. Boris, A. V. Pimenov, A. Maljuk, C. T. Lin, C. Ulrich, and B. Keimer, Phys. Rev. Lett. **92**, 037202 (2004).

[8] R. J. McQueeney, J. Ma, S. Chang, J.-Q. Yan, M. Hehlen, and F. Trouw, Phys. Rev. Lett. **98**, 126402 (2007).

[9] M. Takano, N. Nakanishi, Y. Takeda, S. Naka, and T. Takada, Mater. Res. Bull. **12**, 923 (1977).

[10] P. M. Woodward, D. E. Cox, E. Moshopoulou, A. W. Sleight, and S. Morimoto, Phys. Rev. B **62**, 844 (2000).

[11] I. Yamada, K. Takata, N. Hayashi, S. Shinohara, M. Azuma, S. Mori, S. Muranaka, Y. Shimakawa, and M. Takano, Angew. Chemie Int. Ed. **47**, 7032 (2008).

[12] M. Azuma, W. Chen, H. Seki, M. Czapski, S. Olga, K. Oka, M. Mizumaki, T. Watanuki, N. Ishimatsu, N. Kawamura, S. Ishiwata, M. G. Tucker, Y. Shimakawa, and J. P. Attfield, Nat. Commun. **2**, 347 (2011).

[13] M. Azuma, S. Carlsson, J. Rodgers, M. G. Tucker, M. Tsujimoto, S. Ishiwata, S. Isoda, Y. Shimakawa, M. Takano, and J. P. Attfield, J. Am. Chem. Soc. **129**, 14433 (2007).

[14] Y. Hosaka, F. Denis Romero, N. Ichikawa, T. Saito, and Y. Shimakawa, Angew. Chemie Int. Ed. **56**, 4243 (2017).

[15] A. C. Larson and R. B. Von Dreele, Los Alamos National Laboratory Report LAUR 86-748, 2000 (unpublished).

[16] See Supplemental Material at http://link.aps.org/supplemental/10.1103/PhysRevB.96.064434 for additional discussion regarding the CT transition temperature and refined parameters extracted from the models refined against neutron powder diffraction data as a function of temperature.

[17] A. E. Bocquet, A. Fujimori, T. Mizokawa, T. Saitoh, H. Namatame, S. Suga, N. Kimizuka, Y. Takeda, and M. Takano, Phys. Rev. B **45**, 1561 (1992).

[18] W.-T. Chen, T. Saito, N. Hayashi, M. Takano, and Y. Shimakawa, Sci. Rep. **2**, 449 (2012).

[19] P. D. Battle, T. C. Gibb, and S. Nixon, J. Solid State Chem. **77**, 124 (1988).

[20] J. B. Goodenough, *Magnetism and the Chemical Bond* (Interscience, New York, 1963).

[21] Y. Hosaka, N. Ichikawa, T. Saito, P. Manuel, D. Khalyavin, J. P. Attfield, and Y. Shimakawa, J. Am. Chem. Soc. **137**, 7468 (2015).

[22] T. Takeda, S. Komura, and H. Watanabe, in 3rd International Conference on Ferrites, edited by H. Watanabe, S. Iida, and M. Sugimoto (Japan, 1980), pp 389–392.

[23] M. Mostovoy, Phys. Rev. Lett. **94**, 137205 (2005).

[24] M. Leblanc, G. Ferey, P. Lacorre, and J. Pannetier, J. Magn. Magn. Mater. **92**, 359 (1991).

[25] R. L. White, J. Appl. Phys. **40**, 1061 (1969).

[26] M. Shang, C. Zhang, T. Zhang, L. Yuan, L. Ge, H. Yuan, and S. Feng, Appl. Phys. Lett. **102**, 062903 (2013).

[27] W. Chen, Y. Long, T. Saito, J. P. Attfield, and Y. Shimakawa, J. Mater. Chem. **20**, 7282 (2010).